Structural Eng. / Earthquake Eng. Vol. 6. No. 2, 365s-373s. October 1989
Japan Society of Civil Engineers (Proc. of JSCE No. 410/I-12)

LONG LIFE FATIGUE BEHAVIOR OF FILLET WELDED JOINT IN CORROSIVE ENVIRONMENT

By Masahiro SAKANO, Hiroshi ARAI** and Toshio NISHIMURA****

Long life corrosion fatigue tests were carried out using web-gusset-type fillet welded joints and 3 % NaCl solution. In corrosive environment, fatigue cracks initiated from the bottom of corrosion pits formed along the weld toe and led specimens to failure at such a low stress range as half of the fatigue limit in air and the S_r vs N_f relationship had a linearity with a slope of about $-1/3$ in the range of $N_f=5\times10^5\sim10^7$ cycles on a logarithmic graphpaper. Corrosion fatigue life of fillet welded joints could be accurately estimated by assuming that corrosion pits start to grow from the facet-like initial crack and by using da/dN vs ΔK relationship including corrosion pit growth rate vs ΔK relationship.

Keywords : corrosion fatigue, fillet weld, crack initiation

1. INTRODUCTION

Corrosion fatigue is scarcely considered when setting standards for the design of steel bridges in Japan[1),2)]. However, the fatigue strength of structural steels is known to decrease markedly in corrosive environments[3)]. An adequate understanding of life reduction due to corrosion fatigue is essential in the design and maintenance of steel bridges exposed to corrosive environments such as those by the sea.

Since a number of steel bridges have experienced fatigue cracking at fillet welded joints, it is of great importance to understand the fatigue behavior of these joints more thoroughly. Nishimura and Minata[4)], Yamada and Sadaka[5)], Iwasaki[6)], and Booth[7)] performed corrosion fatigue tests using fillet welded joints. However, little data has been obtained about the low-stress and long-life region which is essential in the fatigue assessment of actual bridge members and little investigation has been made concerning the formation of corrosion pits and the development of fatigue cracks from those pits.

In this study, low-stress and long-life corrosion fatigue tests were carried out at the stress range down to half of the fatigue limit in air and the number of stress cycles up to 10 million. Fillet welded joints with turn-round weldments were used as most fatigue cracks in steel bridges have been found to originate in these parts[8)]. The degree of fatigue life reduction and behavior of fatigue crack development in corrosive environments was investigated and the corrosion fatigue life of welded joints was estimated by applying the fracture mechanics concept.

* Member of JSCE, Dr. Eng., Research Associate, Dept. of Construction Eng., Gunma University (1-5-1, Tenjin-cho, Kiryu-shi, Gunma 376)
** Member of JSCE, M. Eng., Yokogawa Bridge Works, LTD (4-4-44, Shibaura, Minato-ku, Tokyo 108)
*** Member of JSCE, Dr. Eng., Professor, Dept. of Civil Eng., Ashikaga Institute of Technology (268, Omae-cho, Ashikaga-shi, Tochigi 326)

2. FATIGUE TESTS

(1) Specimen

The configurations and dimensions of the specimen with longitudinal attachments are shown in Fig. 1. Since stress concentration occurs due to a three dimensional configuration of the joint in addition to a local one of the weld toe, this type of joint is classified in the category of lowest fatigue strength in the design standard for steel railway bridges[1]. Specimens were made of SM 41 B and SM 58 Q using electrodes of D 5016 and D 5816 respectively. Mechanical properties and chemical composition of the materials are given in Table 1. All the specimens were welded by only one specific welder to make the amount of scatter in weldments as small as possible. The welding conditions are given in Table 2. Neither painting nor coating was conducted supposing the case that the covering material was deteriorated.

(2) Corrosion fatigue tests

Fatigue tests were conducted under tensile cyclic loading with the minimum stress of 9.8 MPa by an electro-hydraulic fatigue testing machine both in air and in a corrosive environment. Considering the effect of briny air, corrosion fatigue tests were performed by pouring 3 % NaCl solution (25±0.5°C, pH=7.1~7.2) on the weld toe at the flow rate of 1 *l*/min. The dissolved oxygen was saturated by aeration. The solution was renewed every one week. Salinity as well as moisture is considered to be a principal cause of corrosion in steel bridges[9),10)] The authors previously reported that salt water reduced fatigue strength more than distilled water and pH=4 H_2SO_4 solution[3]. A corrosion chamber made of acrylic plastic was mounted to the specimen as shown in Fig. 2.

The rate of stress repetition in corrosion fatigue tests was set at 100 cpm (1.67 Hz) in consideration of that of actual live loading in bridge members[3]. In air, fatigue tests were performed at 900 cpm (15 Hz) as the rate of stress repetition has little influence on the fatigue strength.

Table 1 Mechanical Properties and Chemical Composition.

Material	Mechanical Properties			Chemical Composition (%)					
	Y.P. (MPa)	T.S. (MPa)	EL. (%)	C x100	Si x100	Mn x100	P x1000	S x1000	Mo x100
SM41B	304	451	32	12	23	160	20	6	
SM58Q	608	706	25	13	26	141	21	4	
D5016	490	565	31	9	63	90	19	5	
D5816	550	646	28	7	63	110	17	6	24

Table 2 Welding Conditions.

Current (A)	Voltage (V)	Welding speed (cm/min)
150~160	22~23	8

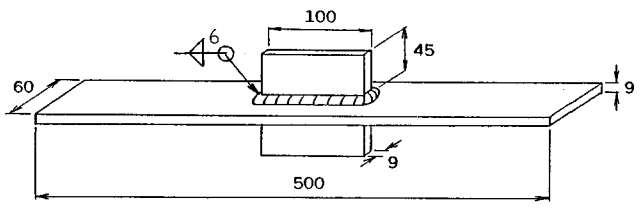

Fig. 1 Fillet Welded Specimen.

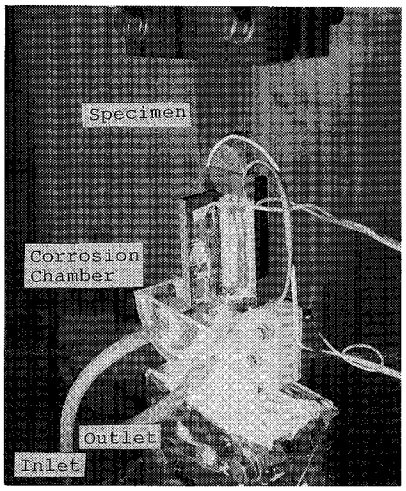

Fig. 2 Corrosion Fatigue Test Set-up.

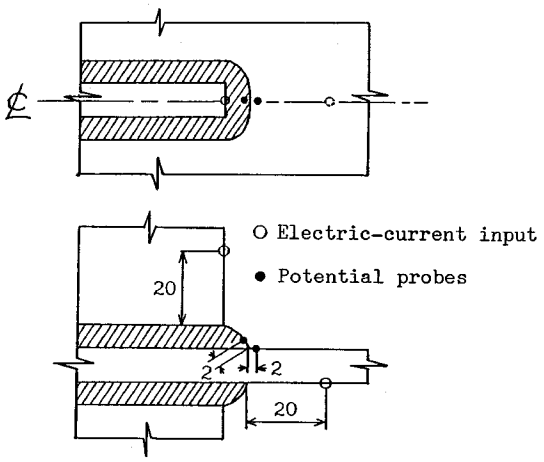

Fig. 3 Location of Electrical Contacts.

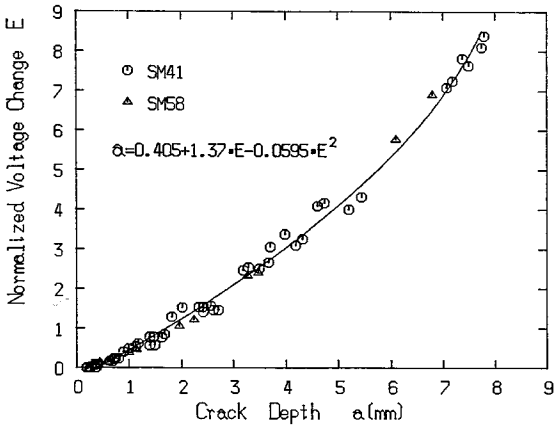

Fig. 4 Relationship between Normalized Voltage Change and Crack Depth.

(3) Detection of fatigue cracks

It is very difficult to mark the crack shape on the crack surface in corrosive environments. Therefore we applied an alternating current potential method to detect fatigue cracks[11),12)]. Fig. 3 illustrates the location of electric current input and potential probes. No cracks initiated at spot weldments of their electrical contacts.

Fig. 4 shows the relationship between normalized voltage change and crack depth obtained by beach mark tests in air. As shown in the figure, crack depth is represented by a quadratic function of normalized voltage change. Fatigue cracks of 0.3~0.5 mm in depth can be detected by use of this method. In this study, crack initiation life N_c is defined as the number of stress cycles when such a small crack is detected.

3. STRESS INTENSITY FACTOR

The stress intensity factor range ΔK for a semi-elliptical surface crack initiated at weld toe is expressed by Eq. (1)

$$\Delta K = S_r\sqrt{\pi a}\cdot F_s\cdot F_g \quad \cdots\cdots (1)$$

where S_r is nominal stress range and a is crack depth. F_s and F_g are correction factors for effects of the crack shape and the finite thickness and width, and nonuniform stresses acting on the crack, respectively. F_s is calculated by Eqs. (2)~(6)[13)],

$$F_s = 1/E(k)(M_1+M_2\cdot\lambda^2+M_3\cdot\lambda^4)\sqrt{\sec(\pi b/2W\cdot\sqrt{\lambda})} \quad \cdots\cdots (2)$$

$$E(k) = \sqrt{1+1.464\,(a/b)^{1.65}} \quad \cdots\cdots (3)$$

$$M_1 = 1.13-0.09\,(a/b) \quad \cdots\cdots (4)$$

$$M_2 = -0.54+0.89/(0.2+a/b) \quad \cdots\cdots (5)$$

$$M_3 = 0.5-1/(0.65+a/b)+14\,(1-a/b)^{24} \quad \cdots\cdots (6)$$

where b is half of the crack surface length, $2W$ is the plate width, and $\lambda = a/T$ (T is the plate thickness). The aspect ratio a/b was assumed to vary with the normalized crack depth a/T. Fig. 5 shows the relationship between a/b and a/T obtained by beach mark tests in air.

F_g can be obtained from stress intensity factor for a crack subjected to the stress distribution occurred when no cracks exist[19)]. Takena et al.[14)] computed the stress distribution without crack by the combination of the coarse-meshed 3-D FEM and the localized 2-D FEM. In this study, the stress analysis of the uncracked joint was carried out by the fine-meshed 3-D FEM[15)]. The toe radius ρ and the toe angle θ were assumed to be 0.5 mm and 60 deg. which are the average values of measured ones near the crack initiation point. Fig. 6 shows the distribution of ρ and θ. No differences are recognized in the shape of the weld toe

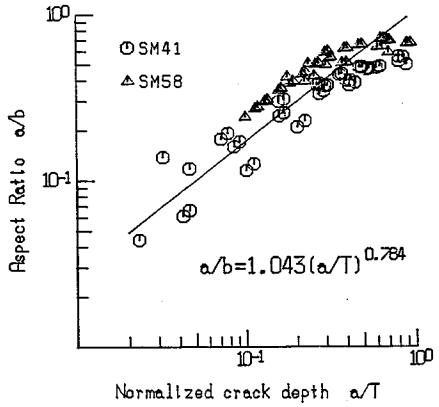

Fig. 5 Change of Crack Aspect Ratio.

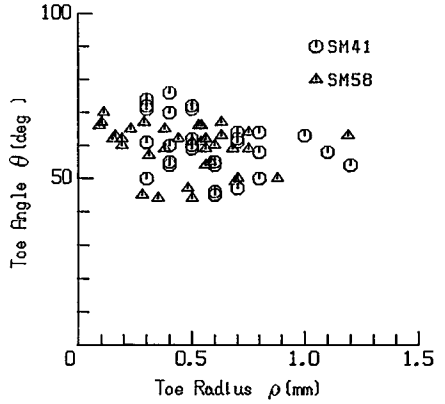

Fig. 6 Distribution of Toe Angle and Toe Radius.

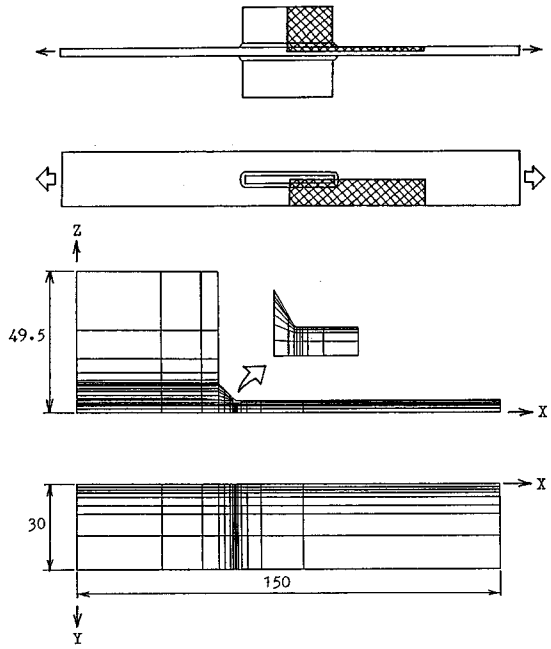

Fig. 7 3-dimensional Finite Element Model.

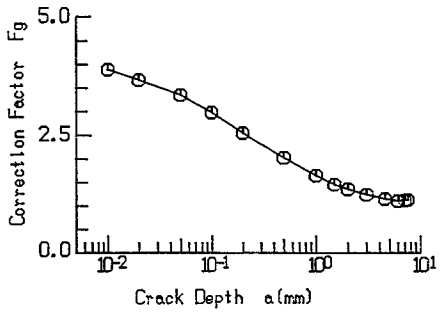

Fig. 8 Change of Correction Factor F_g.

between SM 41 specimens and SM 58 ones. Fig. 7 shows the 3-dimensional finite element model of the fillet welded specimen. One eighth of the whole specimen was analyzed considering its symmetrical configuration. The depth of the smallest element at the weld toe is 0.01 mm. The change of F_g with crack depth is shown in Fig. 8. F_g is 3.7 at the crack depth of 0.02 mm which is assumed to be the initial crack size in estimating fatigue life mentioned in section 6, and decreases rapidly as the crack depth increases.

4. FATIGUE LIFE OF SPECIMENS

(1) Crack initiation life N_c

Fig. 9 shows the relationship between S_r and N_c of specimens. The regression lines in the figure were obtained by the least squares method. In air, fatigue cracks initiated with the number of stress cycles less than 10^6 in the case of S_r more than 100 MPa, whereas no cracks were detected when S_r was less than 90 MPa although the number of stress cycles exceeded 5×10^6. Consequently fatigue limit of 90~100 MPa exists in air regardless of material. In the corrosive environment, fatigue cracks initiated even when S_r was less than the fatigue limit in air and S_r vs N_c lines continued to decline linearly to such a low stress region as half of the fatigue limit.

(2) Fatigue failure life N_f

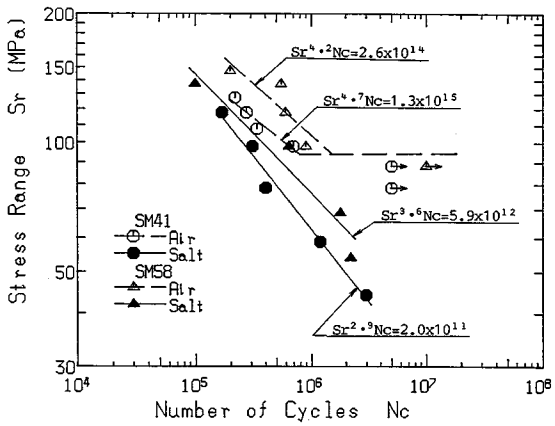

Fig. 9 S_r-N_c Diagram of Specimens.

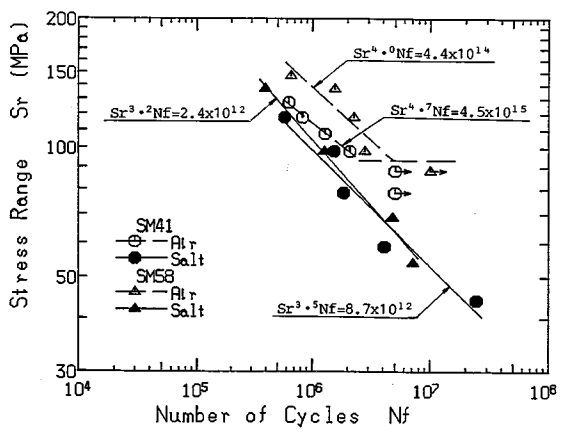

Fig. 10 S_r-N_f Diagram of Specimens.

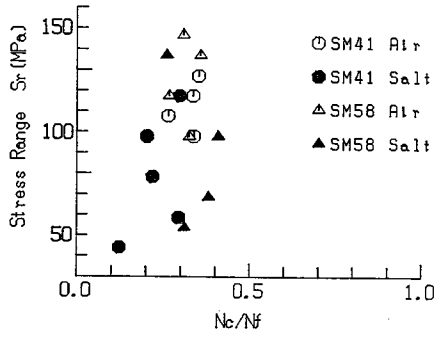

Fig. 11 Ratio of N_c to N_f.

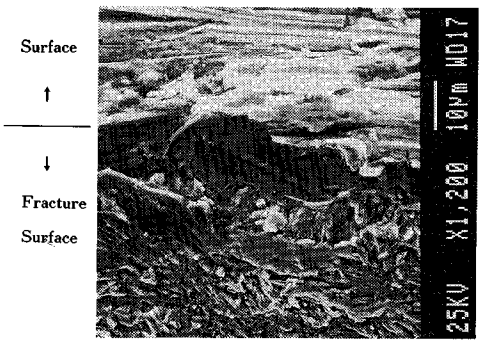

Fig. 12 Scanning Electron Micrograph of Fatigue Fracture Surface (SM 58, S_r=98 MPa, In Air)

The relationship between S_r and N_f (the number of stress cycles to failure) is shown in Fig. 10. The regression lines in the figure were obtained by the least squares method. In air, N_f of SM 58 specimens is longer than that of SM 41 when S_r is higher than the fatigue limit. In a corrosive environment however, such little difference is observed in S_r vs N_f relationship between both materials that S_r vs N_f relationships are expressed by a straight line with the slope of about $-1/3$ on a logarithmic graphpaper even in the long life region of 10^7 cycles.

(3) N_c/N_f

Fig. 11 shows the relationship between N_c/N_f and S_r. The value of N_c/N_f is, independent of S_r, distributed within the range of 0.2~0.4 except for the case of S_r=45 MPa. In that case, an obvious retardation of the crack propagation was caused by the interaction of parallel cracks developed along the weld toe.

Since fatigue cracks initiate at the early stage of fatigue life and most of the fatigue life is occupied by the crack propagation process even in the low stress region as mentioned above, the fracture mechanics concept is effective in the estimation of the corrosion fatigue life.

5. FATIGUE CRACK INITIATION AND PROPAGATION BEHAVIOR

(1) Crack initiation behavior

a) In air

Fatigue cracks initiated at the toe of turn-round weldments. Fig. 12 shows a scanning electron micrograph of fatigue fracture surface near the crack starting point. The facet-like fracture surfaces can

be seen in the vicinity of the surface. These fracture surfaces were observed by Kobayashi et al.[16),17)] and Tanaka and Akiniwa[18)] and are considered to be the stage I crack surface developing at an extremely early stage of fatigue life. Fig. 13 shows the depth of the facet-like fracture surfaces related to the stress range S_r. The depth of them is distributed within 10 μm~30 μm, roughly independent of material and S_r. In this study, we assumed the average value of 20 μm to be the initial crack depth in estimating the fatigue life.

b) In corrosive environment

In corrosive environment, corrosion pits were formed into a groove along the weld toe as shown in Fig. 14 (a). Fatigue cracks initiated at the bottom of them and propagated perpendicular to the loading direction with an increase of stress cycles (see Fig. 14(b)). These pits were observed only in the stress concentrated region along the weld toe. Fig. 15 shows the relationship between stress range S_r and corrosion pit depth measured from fatigue fracture surfaces. The smaller S_r is, the larger the pit depth is. The data of both materials lay between two curves of $\Delta K=3$ and $\Delta K=6$ MPa$\sqrt{\text{m}}$ which were obtained by assuming the pit to be a crack. Since corrosion pits continued to grow to these sizes and fatigue cracks

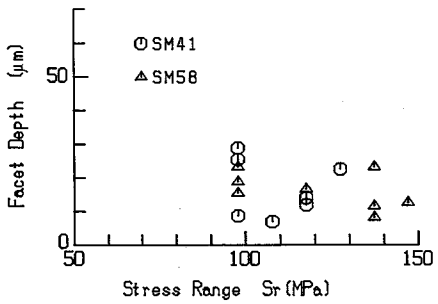

Fig. 13 Depth of Facet-like Fracture Surfaces.

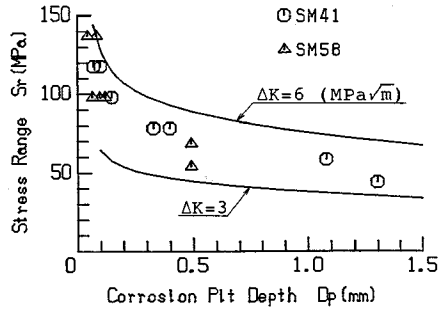

Fig. 15 Relationship between Stress Range and Corrosion Pit Depth.

(a) $N=4\times10^5$ cycles

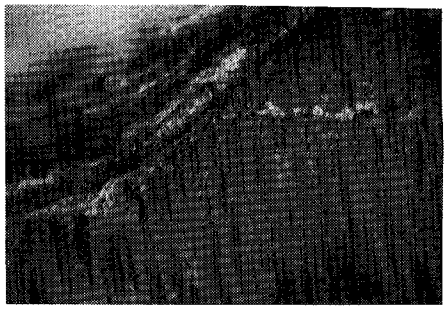

(b) $N=1.15\times10^6$ cycles

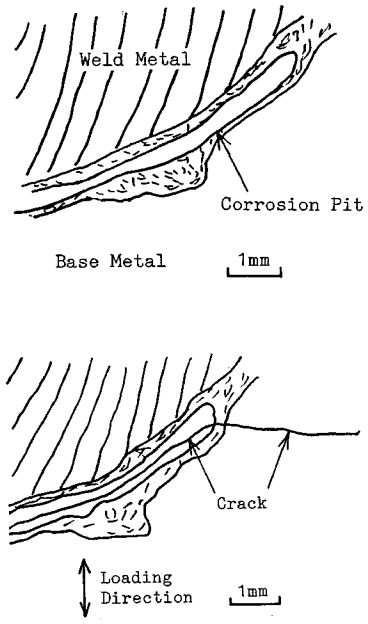

Fig. 14 Corrosion Pit and Fatigue Crack (SM 41, S_r=98 MPa).

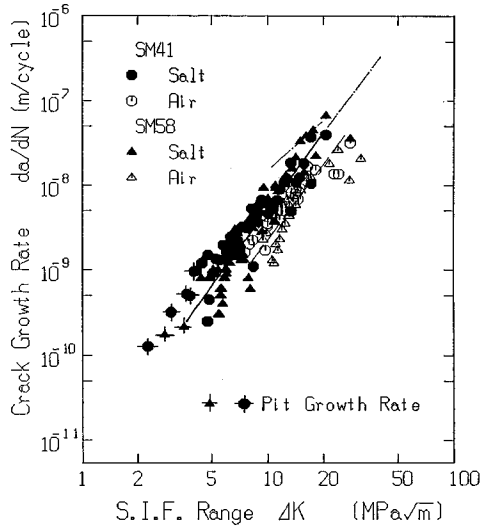

Fig. 16 da/dN vs ΔK Relationship.

started to propagate in succession, this value of ΔK is considered to be a boundary condition between the corrosion pit growth process and the crack propagation one.

(2) Crack propagation behavior

Fig. 16 shows the relationship between crack propagation rate da/dN and stress intensity factor range ΔK in all specimens. The broken line in Fig. 16 indicates the regression line for both materials in air obtained by the least squares method (Eq. (7)) and the solid line indicates that in a corrosive environment (Eq. (8)).

$$da/dN=2.20\times10^{-12}\cdot\Delta K^{3} \quad \cdots\cdots (7)$$

$$da/dN=5.08\times10^{-12}\cdot\Delta K^{3} \quad \cdots\cdots (8)$$

The chain lines in Fig. 16 give the da/dN vs ΔK relationship for SM58 in salt water reported by Yamada and Sadaka[5]. Most data obtained in this study lay in a lower da/dN region than that reported by them.

The corrosion pit growth rate obtained by the AC potential method, for corrosion pits with the depth larger than 0. 4 mm in Fig. 15, is also shown in Fig. 16. As shown in the figure, the relationship between the corrosion pit growth rate and ΔK can be expressed by extension of da/dN vs ΔK line for corrosion fatigue cracks to the lower ΔK region.

6. ESTIMATION OF FATIGUE LIFE

Since fatigue life of fillet welded joints can be considered to be the crack propagation process as mentioned in section 4. (3), the fracture mechanics concept[19] is applied to fatigue life estimation in this study.

(1) In air

Fatigue life N_c and N_f of the specimens were estimated applying da/dN vs ΔK relationship in air expressed by Eq. (7) and $\Delta K_{th}=2.4\ \mathrm{MPa}\sqrt{\mathrm{m}}$ obtained in welded joints[20] and assuming the initial crack depth a_i to be 0. 02 mm which was the average depth of facet-like fracture surfaces shown in Fig. 13. The final crack depth a_f was assumed to be 0. 4 mm in estimation of N_c and 80 % of the plate thickness in that of N_f.

Experimental values and estimation curves of N_c and N_f are shown in Fig. 17 and Fig. 18 respectively. The estimation curves correspond to the experimental values so accurately including those in the vicinity of the fatigue limit, that the assumption of the initial crack depth has been confirmed to be appropriate.

(2) In corrosive environment

In estimation of corrosion fatigue life, da/dN vs ΔK relationship expressed by Eq. (8) obtained in a corrosive environment was applied including the relationship between the corrosion pit growth rate and ΔK and ΔK_{th} was assumed to be zero because fatigue cracks started to propagate from corrosion pits developed along the stress-concentrated weld toe in the low stress region below the fatigue limit in air. The values of a_i and a_f were assumed similarly to those in air.

As shown in Fig. 17 and Fig. 18, the estimation curves closely correspond to the experimental values. Consequently it has been verified that corrosion fatigue life of fillet welded joints can be accurately estimated even in the lower stress region by the fracture mechanics concept taking account of the process of the corrosion pit development.

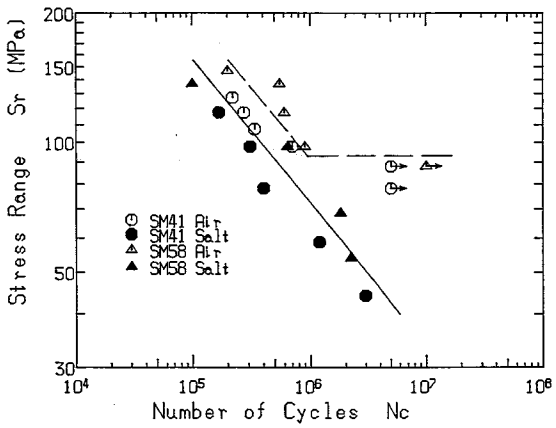

Fig. 17 Estimation of N_c.

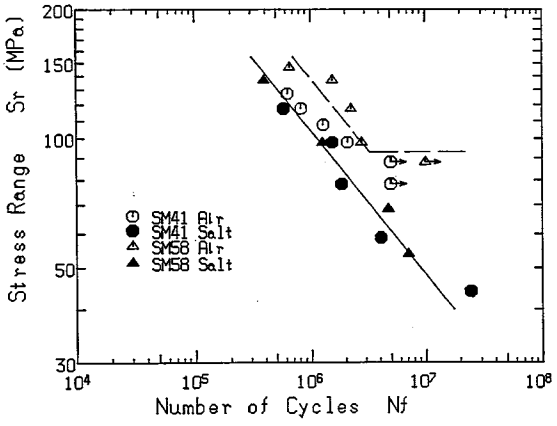

Fig. 18 Estimation of N_f.

7. CONCLUDING REMARKS

In order to investigate long life fatigue behavior of fillet welded joints and the manner of fatigue crack development in corrosive environment, corrosion fatigue tests were carried out at the rate of stress repetition of 100 cpm with emphasis on the low-stress region below the fatigue limit in air. The following are the principal results obtained from this study :

(1) Fatigue limit exists in air, since no fatigue cracks initiated at stress ranges below 90 MPa in both SM 41 and SM 58 specimens. In a corrosive environment, fatigue cracks initiated and led specimens to failure at such a low stress range as half of the fatigue limit in air. And the relationship between the stress range and the number of stress cycles to failure, regardless of the kinds of steel, has the linearity with a slope of about $-1/3$ in the range of $N_f=5\times10^5\sim10^7$ cycles on a logarithmic graphpaper.

(2) On the fracture surface of the specimens failed in air, facet-like portions were observed at the crack initiation point in contact with the surface of the weld toe. The depth of them was 0.01~0.03 mm independent of stress ranges and materials. In a corrosive environment, fatigue cracks initiated from the bottom of corrosion pits formed into a groove along the stress-concentrated portion of the weld toe. The stress intensity factor range ΔK calculated assuming those pits to be cracks was almost constant regardless of the kind of steel and the stress range.

(3) The relationship between fatigue crack growth rate da/dN and ΔK in a corrosive environment can be expressed by a straight line at a slope of 3 on a logarithmic graphpaper putting both data of SM 41 and SM 58 together. In addition, the relationship between corrosion pit growth rate and ΔK can be expressed by extension of da/dN vs ΔK line for corrosion fatigue to the lower ΔK region.

(4) The corrosion fatigue life of fillet welded joints under stress repetition lower than the fatigue limit in air can be accurately estimated by assuming that a corrosion pit starts to grow from the facet-like crack as an initial defect and by using da/dN vs ΔK relationship in a corrosive environment including corrosion pit growth rate vs ΔK relationship.

ACKNOWLEDGMENTS

The authors would like to thank Dr. Chitoshi Miki of Tokyo Institute of Technology, Dr. Yukikazu Tsuji and Mr. Masashi Ikeda of Gunma University for their invaluable advice and assistance. This study was supported by the grant-in-aid for scientific research from the foundation for the promotion of science and technology in Gunma University. Numerical computations for stress analysis were performed at the Computer Center of Gunma University.

REFERENCES

1) JSCE : Standard for Design of Steel Railway Bridges, 1983 (in Japanese).
2) JIR : Specifications for Highway Bridges, 1970 (in Japanese).
3) Sakano, M., Yokoh, M., Arai, H. and Nishimura, T. : Fatigue Crack Initiation Life of Notched Steel Members in Corrosive Environments, Journal of Structural Engineering, Vol. 34 A, pp. 469-481, 1988 (in Japanese).
4) Nishimura, A. and Minata, O. : Surface Irregularity and Fatigue Strength of Gusset Joint under Various Corrosive Environments, Proc. of JSCE, No. 380/ I -7, pp. 401-409, 1987 (in Japanese).
5) Yamada, K. and Sadaka, S. : Fatigue Test of Stiffener Specimens in Salt Water and Life Estimation, Proc. of JSCE, No. 398/ I -10, pp. 377-384, 1988 (in Japanese).
6) Iwasaki, N. : Study on Corrosion Fatigue Strength in Sea Water of Structural Steels and Joints, Doctoral Thesis, Osaka University, 1987 (in Japanese).
7) Booth, G. S. : Constant Amplitude Corrosion Fatigue Strength of Welded Joints, Fatigue in Offshore Structural Steels, Thomas Telford Ltd, pp. 5-16, 1981.
8) Miki, C., Sakano, M., Tateishi, K. and Fukuoka, Y. : Data Base for Fatigue Crackings in Steel Bridges, Proc. of JSCE, No. 392/ I -9, pp. 403-410, 1988 (in Japanese).
9) JSSC : Report of Investigation on Durability of Structures (Railway Bridges), JSSC, Vol. 5, No. 39, pp. 13-15, 1969 (in Japanese).
10) JSSC : Report of Investigation on Durability of Structures (Highway Bridges), JSSC, Vol. 8, No. 84, pp. 6-8, 1972 (in Japanese).
11) Tanaka, K., Akiniwa, Y. and Fujita, S. : AC Electrical Potential Measurement of Fatigue Crack Growth in Notched Specimen, Jour. of JSMS, Vol. 36, No. 401, pp. 177-183, 1987 (in Japanese).
12) Smith, I. F. C. and Smith, R. A. : Fatigue Crack Growth in a Fillet Welded Joint, Engineering Fracture Mechanics, Vol. 18, No. 4, pp. 861-869, 1983.
13) JSMS : Stress Intensity Factors Handbook, Vol. 2, pp. 712-722, Pergamon Press, 1987.
14) Takena, K., Kawakami, H., Itoh, F. and Miki, C. : Stress Analysis and Calculation of Fatigue Lives about Web-Gusset Welded Joints, Proc. of JSCE, No. 392/ I -9, pp. 345-350, 1988 (in Japanese).
15) Wilson, E. L. : A Static Analysis Program for Three Dimensional Solid Structures, Denver Mining Research Center Report, U. S. Department of the Interior Bureau of Mines, 1971.
16) Kobayashi, H., Nakazawa, H. and Komine, A. : Fractographic Study on Stage 1 Crack Propagation Process, Trans. of JSME, Vol. 41, No. 341, pp. 9-21, 1975 (in Japanese).
17) Kobayashi, H., Kawada, Y. and Nakazawa, H. : A Fractographic Study of Stage 1 Cracking with Particular Reference to Endurance Limit, Jour. of JSMS, Vol. 25, No. 276, pp. 881-887, 1976 (in Japanese).
18) Tanaka, K. and Akiniwa, Y. : Resistance-Curve Method for Predicting Propagation Threshold of Short Fatigue Crack at Notches, Engineering Fracture Mechanics, Vol. 30, No. 6, pp. 863-876, 1988.
19) Okamura, H. : Introduction to Linear Fracture Mechanics, Baifukan, 1976 (in Japanese).
20) NRIM : Fatigue Data Sheets, No. 21, 1980, No. 31, 1982 (in Japanese).

(Received April 20 1989)